ELSEVIER

Physica C 307 (1998) 189–196

PHYSICA C

# Structure, microstructure, magnetic properties and chemical stability of $HoBa_2SbO_6$ with $Yba_2Cu_3O_{7-\delta}$ superconductor

J. Albino Aguiar [a,*], C.C. de Souza Silva [a], Y.P. Yadava [a], D.A. Landinez Tellez [a], J.M. Ferreira [a], J. Guzman [b], E. Chavira [b]

[a] *Departamento de Física, Universidade Federal de Pernambuco, 50670-901 Recife, PE, Brazil*
[b] *Instituto de Investigaciones en Materiales, Universidad Autonoma de Mexico, A.P. 70630, 04510 Mexico, DF, Mexico*

Received 23 February 1998; accepted 8 September 1998

**Abstract**

A complex perovskite oxide $HoBa_2SbO_6$ in the Ho–Ba–Hf–O, rare-earth based oxide system, has been synthesised and sintered as a single phase material. The structure, microstructure, quantitative elemental analysis and magnetic properties of this material have been studied by X-ray diffraction, scanning electron microscopy (SEM), energy dispersive X-ray (EDX) techniques and magnetic susceptibility measurements. Significant presence of superstructure reflection lines in the XRD spectra of $HoBa_2SbO_6$ reveals that it is an ordered complex perovskite oxide. Magnetic susceptibility measurements show that $HoBa_2SbO_6$ presents a paramagnetic behaviour at low temperature (5–300 K). Microstructure and EDX analysis show that sintered $HoBa_2SbO_6$ has homogeneous surface morphology with uniform particle size (1–2 μm) distribution and there is no evidence of impurity in the single phase sintered $HoBa_2SbO_6$. The chemical stability of $HoBa_2SbO_6$ with $YBa_2Cu_3O_{7-\delta}$ superconductor was studied. This study shows that $HoBa_2SbO_6$ is chemically compatible with $YBa_2Cu_3O_{7-\delta}$ and it did not have deleterious effect on the superconducting transition temperature of $YBa_2Cu_3O_{7-\delta}$. Also, $HoBa_2SbO_6$ melts congruently and single crystals could be grown from the melt. In view of these favourable characteristics, $HoBa_2SbO_6$ could be used as a potential substrate material for $YBa_2Cu_3O_{7-\delta}$ superconductor film. 

*Keywords:* $HoBa_2SbO_6$; $Yba_2Cu_3O_{7-\delta}$ superconductor; Scanning electron microscopy; Magnetic properties

## 1. Introduction

There are currently immense research interests in perovskite oxide materials containing rare-earth metals. Because of their varied structure, composition, physical and chemical characteristics, these materials have attracted intense research activities in many applied and fundamental areas of solid state science and advanced materials research. Earlier investigations in 1950s and 1960s [1–3] identified a large group of materials which have the basic perovskite $ABO_3$ structure, or a small distortion of that structure. These complex perovskite oxides generally have the formula $A_2BB'O_6$ or $A_3B_2B'O_9$ and result from the ordering of B and B′ cations on the octahedral site of the primitive perovskite unit cell. Due to the increased complexity of unit cell, a large variety of

* Corresponding author. Tel.: +55-81-2718450; Fax: +55-81-2710359; E-mail: albino@npd.ufpe.br

0921-4534/98/$ - see front matter 
PII: S0921-4534(98)00525-5

such materials are possible and hence a more continuous progression of lattice parameter could be produced. Due to the increased flexibility in lattice parameter, complex perovskite oxides have been extensively investigated in recent years as new substrate materials for films of high $T_c$ superconductors [4–7], which are based on the perovskite structure. The increased flexibility in lattice parameter constant in complex cubic perovskites enables a better match of the substrate lattice parameter to that of the high $T_c$ superconductor film.

In view of the above promising characteristics of complex cubic perovskites, we have synthesised and sintered a new ceramic substrate material $HoBa_2SbO_6$, in the rare-earth based Ho–Ba–Sb–O oxide system. We have investigated the substrate characteristics of $HoBa_2SbO_6$ by studying its structure, microstructural and magnetic properties along with the study of chemical stability of $HoBa_2SbO_6$ with $YBa_2Cu_3O_{7-\delta}$ (YBCO) superconductor, for its possible use as substrate. $HoBa_2SbO_6$ was synthesised earlier by Garcia Casado et al. [8,9] and its structure and magnetic properties have been reported in literature. Generally, complex perovskite oxides have the general formula $A_2BB'O_6$ or $A_3B_2B'O_9$ and exhibit order–disorder transition due to the ordering of B and B′ cations on the octahedral sites of the primitive $ABO_3$ perovskite cubic cell. Such an ordering is most probable when large difference exists either in the charges or in the ionic radii of B and B′ cations. Such an ordering phenomenon can be better observed if the difference in scattering power of B and B′ cations is large enough [10,11]. During our study of the structure of $HoBa_2SbO_6$ we observed considerable presence of superstructure reflections in the X-ray diffraction spectrum, which indicate the ordering of Ho and Sb cations on B and B′ sites in $HoBa_2SbO_6$. As the structural ordering is an important factor to understand the electronic behaviour in such materials, we have made a detailed structural characterisation of $HoBa_2SbO_6$ along with the study of various substrate characteristics of this material. In the present work, structural, microstructural studies on $HoBa_2SbO_6$ were made by powder X-ray diffraction (XRD). EDX and scanning electron microscopy (SEM) techniques. Chemical stability of $HoBa_2SbO_6$ with YBCO superconductor was studied by powder X-ray diffraction and magnetic susceptibility measurements on $HoBa_2SbO_6$-YBCO composite samples. These studies and their implications have been presented and discussed in this article.

## 2. Experimental details

### 2.1. Materials synthesis

$HoBa_2SbO_6$ has been synthesised by solid state reaction process. High purity constituent chemicals (purity 99.99%) $Ho_2O_3$, $Sb_2O_3$ and $BaCO_3$ were mixed in stoichiometric ratio and pressed as circular discs (dia. 13 mm, thickness 1 mm). These green body circular discs were calcined at 1100°C for 40 h in ambient atmosphere and slowly cooled down to room temperature. The calcined material was examined by powder X-ray spectrum technique and it showed a multi phase structure. The material was then finely powdered and again pressed as circular discs at a pressure of 5 ton/cm$^2$. These circular discs were heat treated at 1200°C for 24 h. X-ray pattern still showed a mixed phase. We repeated the sintering process again at 1200°C for longer duration (60 h) and finally we obtained a single phase material as evidenced by X-ray diffraction spectrum.

For the study of chemical stability of $HoBa_2SbO_6$ with YBCO superconductor, 0 to 50 wt.% of single phase $HoBa_2SbO_6$ powder was mixed with YBCO superconductor powder. YBCO single phase superconductor powder was prepared by the standard solid state reaction process. YBCO-$HoBa_2SbO_6$ mixed powders were compacted as circular disc at a pressure of 2 ton/cm$^2$ and annealed in oxygen atmosphere at 950°C for 24 h. The samples were cooled down slowly to room temperature.

### 2.2. Materials characterisation techniques

The X-ray diffraction spectra of $HoBa_2SbO_6$, YBCO and YBCO-$HoBa_2SbO_6$ samples were recorded by a Siemens D5000 X-ray diffractometer, using CuK$\alpha$ radiation ($\lambda = 1.5406$ Å). Surface morphology and particle size distribution of the sintered $HoBa_2SbO_6$ were studied by scanning electron microscopy using a Leico-Cambridge model stereoscan 440 electron microscope. Elemental chemistry analysis of $HoBa_2SbO_6$ was made by recording energy-

dispersive X-ray (EDX) spectra of the samples, using a X-ray OXFORD model PENTAFET detector with a Be-window and 128 eV resolution. The accelerating voltage used was 20 kW, the beam current 200 pA and the counting 100 s.

Magnetic properties of $HoBa_2SbO_6$ were studied by measuring magnetic susceptibility in the temperature range 5 to 300 K at 2000 Oe applied magnetic field. Superconductivity in YBCO-$HoBa_2SbO_6$ composites were also studied by measuring magnetic susceptibility of then composite samples in the temperature range 5–300 K. The magnetic susceptibility measurements were carried out using a Quantum Design (MPMS) SQUID magnetometer.

## 3. Results and discussion

### 3.1. Structure

X-ray diffraction (XRD) spectrum of $HoBa_2SbO_6$ synthesised under different processing conditions is shown in Fig. 1. The XRD patterns in Fig. 1 show a clear view of gradual $HoBa_2SbO_6$ phase evolution in Ho–Ba–Sb–O oxide system, under the influence of different processing parameters, i.e., processing temperature and time, of solid state reaction method. The samples processed at 1100°C for 40 h (Fig. 1a) and 1200°C for 40 h (Fig. 1b) contain some extra phase along with the $HoBa_2SbO_6$ phase. Single phase $HoBa_2SbO_6$ (Fig. 1c) was formed only at the processing temperature and time of 1200°C and 60 h

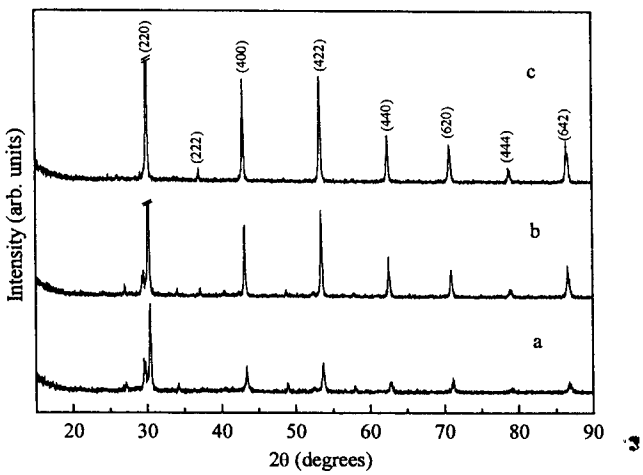


Fig. 1. X-ray diffraction spectrum of $HoBa_2SbO_6$ processed at (a): 1100°C, 40 h; (b) 1200°C, 40 h and (c) 1200°C, 60 h.

respectively. The XRD spectrum of single phase $HoBa_2SbO_6$ (Fig. 1c) is similar to the XRD spectrum of $A_2BB'O_6$ type complex cubic perovskite oxides, e.g., $YBa_2NbO_6$, $GdBa_2SbO_6$, $ErBa_2SbO_6$ reported in JCPDS files and $Ba_2LnSbO_6$ (Ln-lanthanides) materials reported by Garcia Casado et al. [8] As for many perovskites of the general formula $A_2BB'O_6$, an ordered arrangement of B and B′ cations is most probable when large differences exist in either their charges or their ionic radii [10]. This is due to the fact that in a substitutional solid solution BB′, there is random arrangement of B and B′ cations on equivalent position in the crystal structure. If upon suitable heat treatment the random solid solution rearranges into a structure in which B and B′ occupy the same set of positions but in a regular way, such structure is described as superstructure [7,11]. In the superstructure the positions occupied by B and B′ are no longer equivalent and this is exhibited in the XRD spectrum by the presence of superstructure reflection lines.

The ordering phenomenon can be better observed if the differences in scattering power of B and B′ cations are larger enough. In the XRD spectra of single phase $HoBa_2SbO_6$, shown in Fig. 1c, presence of superstructure reflection lines could not be observed clearly, so we recorded slow scan XRD spectra of the same samples with collecting time of 10.0 s and scanning steps of 0.010° and this XRD spectrum of $HoBa_2SbO_6$ is shown in Fig. 2. As seen from Fig. 2, the XRD pattern of $HoBa_2SbO_6$ consists of strong peak characteristics of primitive cubic perovskite plus few weak lines arising from the superlattice. No evidence for a distortion from the cubic symmetry is observed in the XRD data. Only splitting due to $K\alpha_1$, and $K\alpha_2$ radiation is resolved in the $2\theta$ range above 70° (shown in inset of Fig. 2). The significant presence of superstructure reflection lines (111) and (311) clearly reveal the $Ho^{3+}$ and $Sb^{3+}$ cations ordering on B and B′ positions in $A_2BB'O_6$ structure of $HoBa_2SbO_6$. The basic perovskite composition is $ABO_3$, where A is a large ion suitable to the 12 coordinated cube octahedral sites and B is a smaller ion suitable to the 6-coordinated octahedral site. Complex perovskite with mixed species on a site (particularly the B site) may be represented by multiples of this formula unit and larger unit cell. Thus in $HoBa_2SbO_6$, $Ba^{2+}$ cation

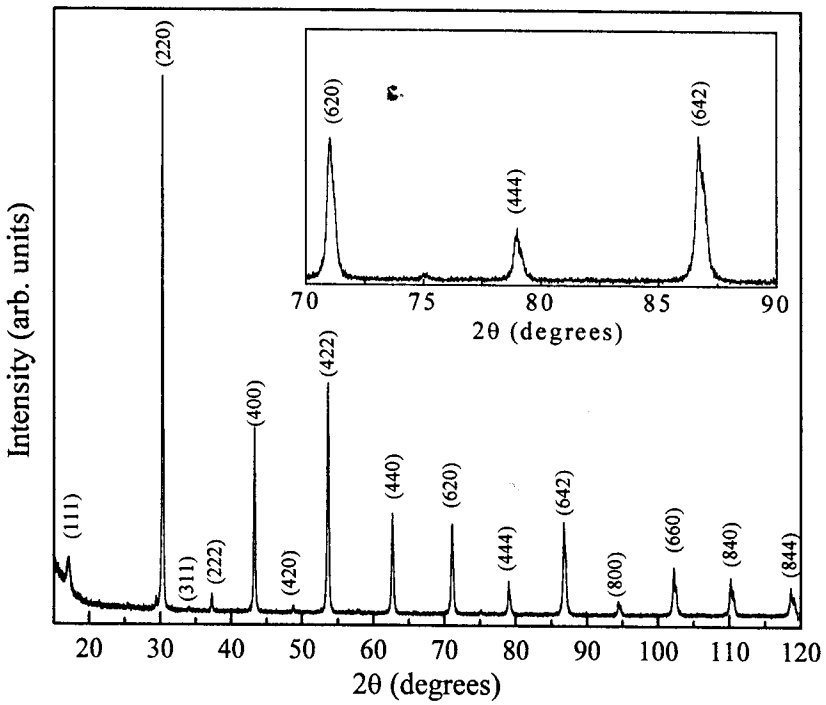


Fig. 2. X-ray diffraction spectrum of single phase $HoBa_2SbO_6$.

(ionic radius 1.34 Å) with the largest ionic radius in this composition, occupies A position and $Ho^{3+}$ (ionic radius 0.89 Å) and $Sb^{3+}$ (ionic radius 0.76 Å) cations occupy B position due to their smaller ionic radii compared to that of $Ba^{2+}$ cation.

Due to the ordering of B and B′ cations on octahedral site of the primitive $ABO_3$ unit cell, there is doubling in the lattice parameter of the basic cubic perovskite unit cell. Based on above considerations, we have indexed the XRD peaks of $HoBa_2SbO_6$ as an ordered complex cubic $A_2BB'O_6$ crystal structure. XRD data of $HoBa_2SbO_6$, obtained from the XRD spectrum are tabulated in Table 1. The lattice constant of $HoBa_2SbO_6$ calculated from $d$ values is 8.3712 Å.

Based on the ionic radii as given is Shannon and Prewitt [12] and using a hard sphere approximation, an average value of the lattice parameter $a_{cal}$ may be calculated theoretically using the relation

$$a_A = 2(R_A + R_0)/\sqrt{2} \quad (1)$$

$$a_B = R_B + R_{B'} + 2R_0 \quad (2)$$

and

$$a_{cal} = (a_A + a_B)/2 \quad (3)$$

where $R_A$, $R_B$, $R_{B'}$ and $R_0$ are the ionic radii of the respective cations A, B, B′ and of the anion oxygen. $a_A$ and $a_B$ are the calculated lattice parameters based on A and B cations, $a_{cal}$ is the average calculated lattice parameter. Using relations (1), (2) and (3), we obtained an average value of the lattice constant $a_{cal}$

Table 1
X-ray diffraction data of $HoBa_2SbO_6$

| $2\theta$ | $d$ (Å) | $I/I_0$ | $hkl$ |
|---|---|---|---|
| 17.040 | 5.1992 | 10.90 | 111 |
| 30.269 | 2.9503 | 100.00 | 220 |
| 34.042 | 2.6315 | 1.61 | 311 |
| 37.234 | 2.4128 | 4.25 | 222 |
| 43.227 | 2.0912 | 35.31 | 400 |
| 48.753 | 1.8663 | 2.06 | 420 |
| 53.559 | 1.7096 | 43.44 | 422 |
| 62.637 | 1.4819 | 19.46 | 440 |
| 71.012 | 1.3263 | 17.43 | 620 |
| 78.976 | 1.2113 | 6.01 | 444 |
| 86.710 | 1.1220 | 17.06 | 642 |
| 94.410 | 1.0497 | 3.01 | 800 |
| 102.164 | 0.9900 | 9.35 | 660 |
| 110.137 | 0.9396 | 7.56 | 840 |
| 118.556 | 0.8960 | 5.37 | 844 |

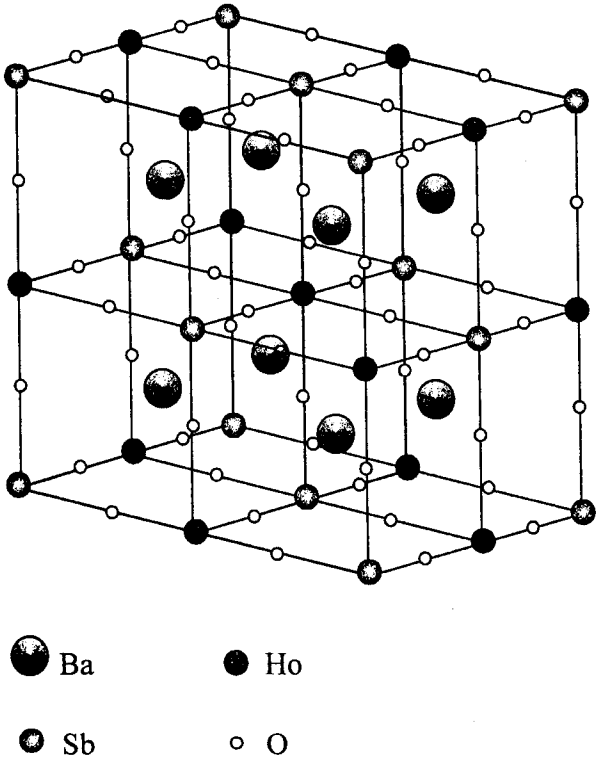


Fig. 3. Crystal structure diagram of $HoBa_2SbO_6$.

of $HoBa_2SbO_6$ of 8.0558, which is 3.9% smaller than the experimental value of $a = 8.3712$ Å. Similar differences have been observed in experimental and theoretical values of lattice parameter in some other $A_2BB'O_6$ type perovskite oxides such as $YBa_2NbO_6$, $DyBa_2SbO_6$, etc. Taking into account the doubling of the basic perovskite unit cell of $HoBa_2SbO_6$, the complex cubic ordered perovskite structure of this material is represented in Fig. 3. These results are in agreement with the earlier structural studies made on $HoBa_2SbO_6$ [8,9].

### 3.2. EDX and surface morphology

Energy dispersive X-ray (EDX) analysis was performed on the single phase $HoBa_2SbO_6$ for the quantitative elemental chemistry analysis. The results of EDX analysis are presented in Table 2. As seen from Table 2 there is no evidence of impurity traces in the samples. Surface morphology of sintered $HoBa_2SbO_6$ was investigated by scanning electron microscopy (SEM). The results are shown in the micrograph, Fig. 4. It indicates that the surface of the

Table 2
Quantitative elemental analysis data of $HoBa_2SbO_6$ obtained by EDX analysis

| Element | Element % | Atomic % |
|---|---|---|
| Ho | 20.14 | 7.05 |
| Sb | 21.26 | 10.09 |
| Ba | 40.35 | 16.91 |
| O | 18.26 | 65.90 |
| Total | 100.00 | 100.00 |

sample presents a crystallinity, which is typical of a polycrystalline ceramic material. The SEM micrograph shows homogeneous surface morphology and particle size distribution. The average of the particle size was estimated to be 1–2 μm.

### 3.3. Magnetic properties

The magnetic properties of $HoBa_2SbO_6$ have been investigated by measuring the dc magnetic susceptibility of $HoBa_2SbO_6$ in the temperature range 5 to 300 K and at an applied magnetic field of 20 kOe. Fig. 5 shows the temperature dependence of the magnetic susceptibility vs. temperature curve for $HoBa_2SbO_6$. The magnetic susceptibility data of Fig. 5 can be fitted well with the Curie–Weiss law,

$$\chi = \chi_0 + C/(T - \theta_p) \quad (4)$$

where $C$ is the Curie constant ($C = N\mu_{\text{eff}}^2/3K$), $N$ is Avogadro's number, $\mu_{\text{eff}}$ is the effective magnetic

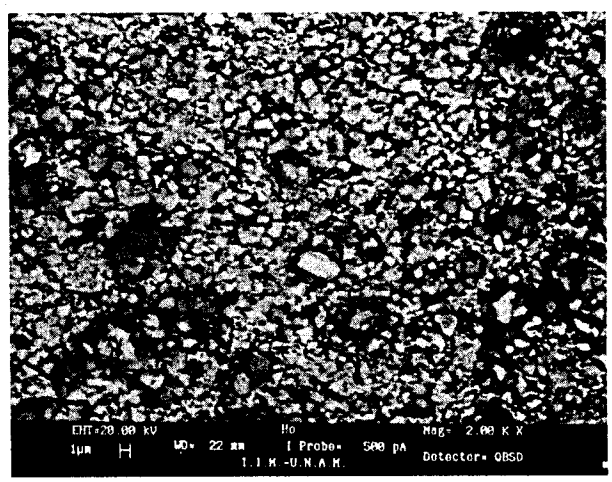


Fig. 4. Scanning electron micrograph of single phase $HoBa_2SbO_6$ sintered at 1200°C for 60 h.

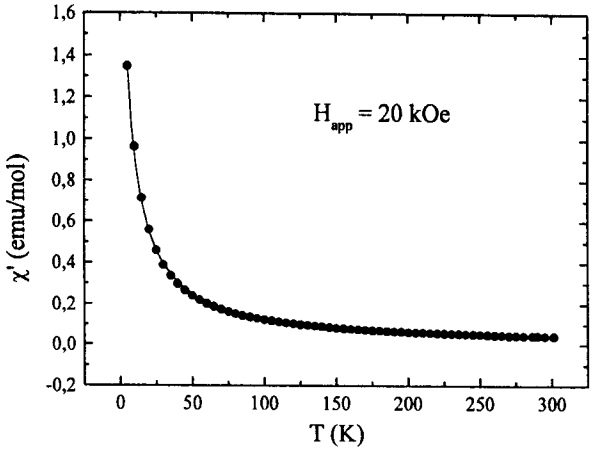


Fig. 5. Dc magnetic susceptibility vs. temperature curve for $HoBa_2SbO_6$.

moment ($\mu_{eff} = P_{eff}\,\mu_B$), $P_{eff}$ is the effective Bohr magneton number, $\mu_B$ is the Bohr magneton, $K$ is Boltzmann constant, $\theta_p$ is the paramagnetic Curie temperature and $\chi_0$ is the temperature independent susceptibility term.

The magnetic parameters for $HoBa_2SrO_6$, extracted from the Curie–Weiss law (Fig. 6) are tabulated in Table 3. The value of the temperature independent susceptibility term $\chi_0$ is $9.82 \times 10^{-3}$ emu/mol. Fig. 6 shows the reciprocal susceptibility $(\chi - \chi_0)^{-1}$ as a function of temperature with $\chi_0 = 9.82 \times 10^{-3}$ emu/mol. The Curie constant, estimated from the solid line in Fig. 6 is $C = 14.44156$ emu K/mol. The effective magnetic moment per Ho

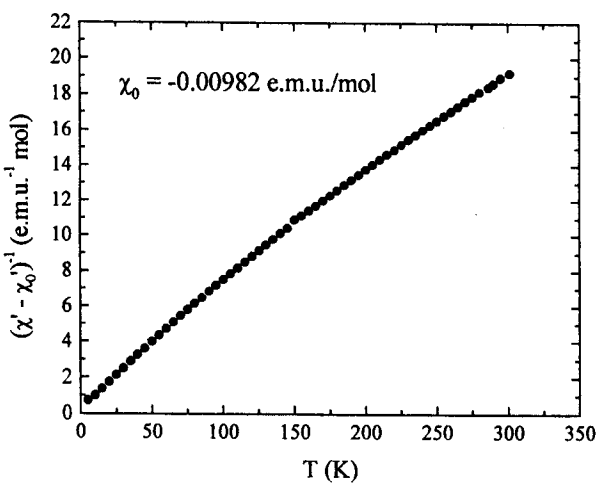


Fig. 6. $(\chi - \chi_0)^{-1}$ vs. temperature curve for $HoBa_2SbO_6$. The solid line shows a fitted Curie–Weiss line.

Table 3
Curie–Weiss parameters for $Ho^{3+}$ in $HoBa_2SbO_6$, determined from the magnetic dc susceptibility measurements

| Parameters | Value | Error |
|---|---|---|
| $C$ (emu K/mol) | 14.44156 | 0.19661 |
| $\theta$ (K) | −5.46854 | 0.16451 |
| $\chi_0$ (emu/mol) | −0.00982 | 0.00188 |

ion, calculated from the Curie constant is $10.74\mu_B$. This is slightly higher than that of the spin-only moment ($10.60\mu_B$) expected for an isolated $Ho^{3+}$ ion and the effective moment of $Ho^{3+}$ in $HoBa_2SbO_6$ obtained by Alonso et al. [9]. This may be due to the crystal field effects of the trivalent $Ho^{3+}$ cation, shown to explain the magnetic susceptibility in this compound.

### 3.4. $YBa_2Cu_3O_{7-\delta}$–$HoBa_2SbO_6$ composites: chemical stability

In order to verify the possibility of using $HoBa_2SbO_6$ as a substrate material for thin film of YBCO superconductor, we have studied the chemical reactivity of $HoBa_2SbO_6$ with YBCO. Appropriate amounts of $HoBa_2SbO_6$ (0 to 50 wt.%) were mixed with YBCO, pelletised and heat treated at 950°C for 24 h in oxygen atmosphere. The YBCO-$HoBa_2SbO_6$ composite samples were finally slowly cooled down to room temperature. X-ray diffraction patterns of these composites are shown in Fig. 7, for 0 to 50 wt.% addition of $HoBa_2SbO_6$ in YBCO. As seen from Fig. 7, all the peaks in the XRD could be indexed either for YBCO or for $HoBa_2SbO_6$ and no extra XRD peak. Within the accuracy of X-ray diffraction technique, these results show that YBCO and $HoBa_2SbO_6$ remain as two distinct separate phases in the YBCO-$HoBa_2SbO_6$ composites and $HoBa_2SbO_6$ is chemically stable with YBCO superconductor even up to 50 wt.% addition of $HoBa_2SbO_6$ in YBCO and heat treated at 950° for 24 h.

### 3.5. Superconductivity in $YBa_2Cu_3O_{7-\delta}$–$HoBa_2SbO_6$ composites

The superconductivity in YBCO-$HoBa_2SbO_6$ composite samples was studied by measuring the ac

magnetic susceptibility of the composites in a frequency of 31 Hz, ac field of 0.1 Oe and in the temperature range 5 to 300 K. Fig. 8 shows the real part of the ac magnetic susceptibility vs. temperature curves for the YBCO-$HoBa_2SbO_6$ composites with 0 to 50 wt.% of $HoBa_2SbO_6$ addition in YBCO superconductor. As seen from the Fig. 8 all the YBCO-$HoBa_2SbO_6$ composites have the same superconducting transition temperature $T_c = 92$ K as that of the pure YBCO superconductor. This shows that even up 50 wt.% of $HoBa_2SbO_6$, an insulating ceramic oxide, addition in YBCO did not have any deteriorating effect on the superconducting transition of YBCO superconductor. Thus as discussed earlier $HoBa_2SbO_6$ is chemically stable with YBCO superconductor and at the same time it did not have any deteriorating effect on the superconducting transition temperature of YBCO.

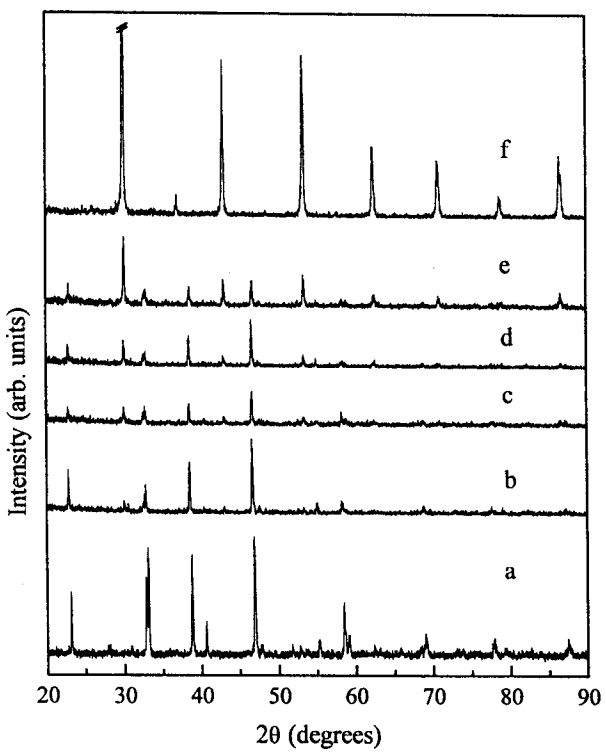


Fig. 7. X-ray diffraction spectrum of $YBa_2Cu_3O_{7-\delta}$–$HoBa_2SbO_6$ composites with: (a) 0 wt.%, (b) 10 wt.%, (c) 20 wt.%, (d) 30 wt.% and (e) 50 wt.% $HoBa_2SbO_6$ in the composite, and (f) pure $HoBa_2SbO_6$.

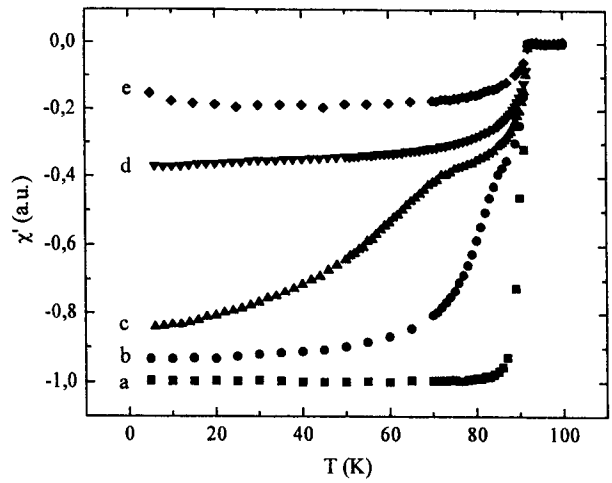


Fig. 8. Real part of the ac magnetic susceptibility vs. temperature curves for $YBa_2Cu_3O_{7-\delta}$–$HoBa_2SbO_6$ composites with (a): 0 wt.%, (b) 10 wt.%, (c) 20 wt.%, (d) 30 wt.% and (e) 50 wt.% $HoBa_2SbO_6$ in the composite.

### 3.6. Congruent melting of $HoBa_2SbO_6$

As single crystals are needed for substrate applications, melting experiment on $HoBa_2SbO_6$ was carried out to examine whether this material melts congruently for its possible single crystal growth from the melting. $HoBa_2SbO_6$ powder was placed in a platinum crucible and this powder was melted completely in air at a temperature of ~ 1750°C. The melted material was slowly cooled down to room temperature and examined by XRD technique. The XRD spectrum of melted material is identical to that of the single phase $HoBa_2SbO_6$, recorded before the melting experiment. This study shows that $HoBa_2SbO_6$ melts congruently and could be grown as single crystals for substrate applications.

## 4. Conclusions

In conclusion, we have synthesised and sintered $HoBa_2SbO_6$ as a single phase material by solid state reaction technique. The structural study by X-ray diffraction technique shows that it is an ordered complex cubic perovskite with lattice constant $a =$ 8.3712 Å. EDX analysis shows that there is no evidence of impurity in the synthesised material and scanning electron micrograph shows the homogeneous surface morphology and uniform particle size distribution with particle size 1–2 μm. $HoBa_2SbO_6$

shows paramagnetic Curie Weiss behaviour at low temperature and effective magnetic moment of $Ho^{3+}$ ion in $HoBa_2SbO_6$ is $10.74\mu_B$. Chemical stability studies made on $YBa_2Cu_3O_{7-\delta}$–$HoBa_2SbO_6$ composites show that $HoBa_2SbO_6$ is chemically compatible with $YBa_2Cu_3O_{7-\delta}$ superconductor and at the some time it did not have any deteriorating effect on the superconducting transition temperature of YBCO superconductor. $HoBa_2SbO_6$ melts congruently and could be grown as single crystals from the melt. These favourable characteristics make $HoBa_2SbO_6$ a promising substrate material for the production of $YBa_2Cu_3O_{7-\delta}$ superconductor films.

## Acknowledgements

This work was financed by Brazilian Science Agencies CNPq and FINEP.

## References

[1] R. Roy, J. Am. Ceram. Soc. 37 (1994) 581.
[2] F. Galasso, L. Katz, R. Ward, J. Am. Ceram. Soc. 81 (1959) 820.
[3] F. Galasso, J.R. Borrante, L. Katz, J. Am. Ceram. Soc. 83 (1961) 2830.
[4] C.D. Brandle, V.J. Fratello, J. Mater. Res. 5 (1990) 2160.
[5] J. Koshy, K.S. Kumar, J. Kurian, Y.P. Yadava, A.D. Damodaran, J. Am. Ceram. Soc. 78 (1995) 3088.
[6] I.T. Kim, Y.H. Kim, S.J. Chung, Jpn. J. Appl. Phys. 34 (1995) 4096.
[7] V.J. Fratello, C.W. Berkstresser, C.D. Brandle, A.J. Van Graitis, J. Cryst. Growth 166 (1996) 878.
[8] P. Garcia Casado, A. Mendiola, I. Rasines, Z. Anorg. Allg. Chem. 510 (1984) 194.
[9] J.A. Alonso, C. Cascales, P. Garcia Casado, I. Rasines, J. Solid State Chem. 128 (1997) 247.
[10] W.T. Fu, D.J.W. Ijdo, J. Solid State Chem. 128 (1997) 323.
[11] A.F. Wells, Structural Inorganic Chemistry, 5th edn. Clarendon Press, Oxford, UK, p. 279, 1986.
[12] R.D. Shannon, C.T. Prewitt, Acta. Cryst. B 25 (1969) 925.